Chemico-Biological Interactions 206 (2013) 289–301

Contents lists available at ScienceDirect

Chemico-Biological Interactions

journal homepage: www.elsevier.com/locate/chembioint

Biological evaluation of morin and its new oxovanadium(IV) complex as antio-xidant and specific anti-cancer agents

Luciana G. Naso [a], Luis Lezama [b], Teófilo Rojo [b], Susana B. Etcheverry [a,c], María Valcarcel [d], Meritxell Roura [d], Clarisa Salado [d], Evelina G. Ferrer [a], Patricia A.M. Williams [a,*]

[a] Centro de Química Inorgánica (CEQUINOR, CONICET, UNLP), Departamento de Química, Facultad de Ciencias Exactas, Universidad Nacional de La Plata, 47 y 115, CC 962 (B1900AVV), 1900 La Plata, Argentina
[b] Departamento de Química Inorgánica, Facultad de Ciencia y Tecnología, Universidad del País Vasco, Apdo 644, 48080 Bilbao, Spain
[c] Cátedra de Bioquímica Patológica, Facultad de Ciencias Exactas, Universidad Nacional de La Plata, 47 y 115, 1900 La Plata, Argentina
[d] Innoprot SL, Edificio 502, P1, Parque Tecnológico, 48160 Derio, Spain

ARTICLE INFO

Article history:
Received 15 May 2013
Received in revised form 14 September 2013
Accepted 5 October 2013
Available online 11 October 2013

Keywords:
Natural antioxidant morin
Oxovanadium(IV) complex
Radical scavengers
Tumor specificity

ABSTRACT

It is known that flavonoids possess, among others, antioxidant and antitumoral properties that depend on their molecular structure. The central objective if this study was to investigate the potential antioxidant and antiproliferative properties of the flavonol morin and its new oxovanadium(IV) complex (VOmor) that was synthesized in order to modify the morin chemical structure. Two osteoblast (UMR106 and MC3T3E1), two breast tumor (T47D and SKBR3) and breast epithelial cell lines in culture were used for the antitumoral determinations. Additionally, a comparative study of their antioxidant capacities using different radicals (DPPH·, $ABTS^{+\cdot}$, OH·, O_2^{-}, ROO·) was performed. Selected mechanisms of action were studied using the breast cancer cell lines. Results obtained show that morin and its complex behaved as good antioxidant agents for some of the radicals and that the complexation improved the behavior with respect to OH· and O_2^{-} radicals being morin more effective as ROO· scavenger. A considerable variation in sensitivity was observed in the breast cancer cells but non-specificity was found for the treatment of osteosarcoma. Moreover, the compounds did not affect the normal proliferation of the breast epithelial mammal cells. The mechanistic studies demonstrated that the complex did not generate reactive oxygen species in the cells (confirming the *in vitro* studies) and did not produce any damage of DNA. The plasmatic membrane was observed to be damaged only in the SKBR3 cell line. In contrast, the perturbation of the mitochondrial membrane potential and the activation of caspase 3/7 for the breast tumor cells revealed an apoptotic cell death process. All these results collectively suggested that VOmor complex could serve as promising pharmacologically active substance against breast cancer treatment.

1. Introduction

Flavonoids are a group of low-molecular-weight polyphenolic substances [1]. They occur naturally in fruit, vegetables, nuts, seeds, flowers, and bark and are an integral part of the human diet. The biochemical activities of flavonoids and their metabolites depend on their chemical structure and the relative orientation of various moieties on the molecule. The major flavonoid classes include flavonols, flavones, flavanones, catechins (or flavanols), anthocyanidins, isoflavones, dihydroflavonols, and chalcones [2]. Morin [2-(2′,4′-dihydroxyphenyl)-3,5,7-trihydroxy-4H-1-benzopyran-4-one], is a flavonoid that has been identified in fruits, vegetables, tea, wine, and many Oriental medicinal herbs. It is a yellow pigment isolated from plants of the Moraceae family [3] and consists of two aromatic rings which are linked by an oxygen-containing heterocycle (ring C) (Fig. 1) [4].

Abundant in the human diet, with potent antioxidant and metal ion chelating capacity, morin possesses several biological and biochemical effects including antiinflammatory, antineoplastic and cardioprotective activities [5]. Potential alternatives to synthetic phenolics being commonly used for the food industry, morin

Abbreviations: AAPH, 2,2-azobis(2-amidinopropane) dihydrochloride; ABTS, 2,2′-azinobis(3-ethylbenzothiazoline-6-sulfonic acid) diammonium salt; CM-H2DCFDA, 5-(and-6)-chloromethyl-2,7,dichlorodihydrofluorescein diacetate acetyl ester; DAPI, 4′,6′-diamidino-2-phenylindole; DHR123, dihydrorhodamine 123; DMEM, Dulbecco's modified Eagle's medium; DMSO, dimethyl sulfoxide; DPPH·, 1,1-diphenyl-2-picrylhydrazyl radical; FBS, fetal bovine serum; H2AX, subtype of H2A histone; LDH, lactate dehydrogenase; MTT, 3-(4,5-methyl-thiazol-2-yl)-2,5diphenyl-tetrazolium bromide; NBT, nitroblue tetrazolium; PBS, phosphate-buffered saline; ROI, regions-of-interest; ROS, reactive oxygen species; SOD, superoxide dismutase; TEAC, Trolox equivalent antioxidant coefficient; TMRM, tetramethyl rhodamine methyl ester; Trolox, 6-hydroxy-2,5,7,8-tetramethylchroman-2-carboxylic acid; VOmor, $[VO(mor)_2H_2O]\cdot 5H_2O$.

* Corresponding author. Tel./fax: +54 0221 4259485.
E-mail address: williams@quimica.unlp.edu.ar (P.A.M. Williams).

0009-2797/$ - see front matter © 2013 Elsevier Ireland Ltd. All rights reserved.
http://dx.doi.org/10.1016/j.cbi.2013.10.006

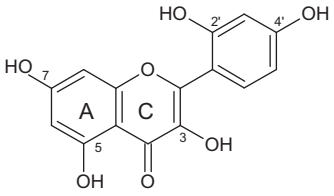

Fig. 1. Structure of morin.

may also have healthy benefits. Epidemiological studies already have indicated that adequate intakes of flavonoid-rich foods may reduce the risk of coronary heart disease and certain cancers [6,7]. The antioxidant properties of morin are directed to scavenge superoxide anions and highly reactive species involved in the initiation of lipid peroxidation. On the other hand, as a phenolic compound, morin may act as an antioxidant compound through the chelation of low valent metal ions such as Fe^{2+} or Cu^{2+} and the regeneration of membrane bound antioxidants such as R-tocopherol [4]. Furthermore, morin can modulate the activities of the metabolic enzymes, including cytochrome P450 and protect various human cells, like myocytes, endothelial cells, hepatocytes and erythrocytes, against oxidative damages. Moreover, morin acts as a chemopreventive agent against oral carcinogenesis in *in vitro* and *in vivo* studies [8].

Vanadium is considered a trace metal possessing antitumor effects when administered at proper concentrations in experimentally-induced tumors [9]. Vanadium compounds have been found to be potentially effective against murine leukaemia, fluid and solid Ehrlich ascites tumour, murine mammary adenocarcinoma and HEp-2 human epidermoid carcinomal cells and human lung, breast, and gastrointestinal tract carcinomas [10]. On the other hand, vanadium tetravalent compounds proved to be genotoxic in several *in vitro* systems, inducing micronuclei and chromosomal aberrations in human peripheral blood cells, and causing guanosine hydroxylation and DNA-strand breaks through the generation of free radicals [11].

In the present study, we aimed to investigate the antioxidant and anticancer activity of morin and also intend to obtain an improvement of these capacities introducing a structural modification of the flavonoid by chelation to a metal center. We have synthesized a new coordination compound of morin and oxovanadium(IV) cation. The complex was characterized by means of elemental analysis, UV–vis, EPR, and Fourier transform infrared (FTIR) spectroscopies and thermal degradation analysis. Their antioxidant properties were assayed *in vitro* and the antiproliferative effects, morphological changes and ROS generation in normal (mouse) and tumoral (rat) bone cell lines in culture were investigated. It is a well-known fact that tumor evolution toward metastasis involved a multistage process in which malignant cells reach distant organs. In this context, investigators challenges consist in recreate the chemical scenario as model of study. It has been established that metastasis to bone occurs most frequently in breast cancer and therefore, it is important to evaluate the cytotoxic effect of the complex in breast cancer cell lines [12] and to determine the specificity of the compounds. Different assays using human normal and tumoral breast cell lines in culture were performed. The most sensitive breast cancer lines were selected to study their possible mechanism of action. In this context, the disruption of the mitochondrial membrane potential, ROS generation, caspase 3/7 activation and histone phosphorilation were investigated. In a previous paper [13] a partially characterized $V(IV)O^{2+}$ morin complex was reported. The difference in the synthesis and the physicochemical properties of that binuclear compound allow us to conclude that the binuclear complex is different from the mononuclear VOmor reported and characterized herein.

2. Materials and methods

2.1. Materials

Morin hydrate (Fluka), oxovanadium(IV) chloride (50% aqueous solution, Carlo Erba), and solid oxovanadium(IV) sulfate pentahydrate (Merck) were used as supplied. Corning or Falcon provided tissue culture materials. Dulbecco's modified Eagle's medium (DMEM), and trypsin–ethylenediaminetetraacetic acid (EDTA) were purchased from Gibco (Gaithersburg, MD, USA), and fetal bovine serum (FBS) was from GibcoBRL (Life Technologies, Germany). All other chemicals used were of analytical grade. Endotoxin-free RPMI and endotoxin-free Mc Coy medium were from Sigma–Aldrich (St. Louis, MO).

2.2. Physicochemical characterization

Elemental analysis for carbon and hydrogen was performed using a Carlo Erba EA1108 analyzer. Vanadium content was determined by the tungstophosphovanadic method [14]. Thermogravimetric analysis and differential thermal analysis were performed with Shimadzu systems (models TG-50 and DTA-50, respectively), working in an oxygen flow of 50 mL min^{-1} and at a heating rate of 10 °C min^{-1}. Sample quantities ranged between 10 and 20 mg. Al_2O_3 was used as a differential thermal analysis standard. UV–vis spectra determinations were recorded with a Hewlett–Packard 8453 diode-array spectrophotometer. The diffuse reflectance spectrum was recorded with a Shimadzu UV-300 spectrophotometer, using MgO as a standard. Infrared spectra were measured with a Bruker IFS 66 FTIR spectrophotometer from 4000 to 400 cm^{-1} using the KBr pellet technique. A Bruker ESP300 spectrometer operating at the X-band and equipped with standard Oxford Instruments low-temperature devices (ESR900/ITC4) was used to record the spectrum of the complex at room temperature in the solid state. Anisotropic X-band EPR spectra of frozen solutions were recorded at 150 K, after addition of 5% DMSO to ensure good glass formation. A computer simulation of the EPR spectra was performed using the program WINEPR SimFonia (version 1.25, Bruker Analytische Messtecnik, 1996). Fluorescence spectra were obtained using a Perkin Elmer (Beaconsfield, UK) LS-50B luminescence spectrometer equipped with a pulsed xenon lamp (half peak height less than 10 μs, 60 Hz), an R928 photomultiplier tube, and a computer working with FLWinlab.

2.3. Synthesis of $[VO(mor)_2H_2O]\cdot 5H_2O$ (VOmor)

A 50% aqueous solution of $VOCl_2$ (0.25 mmol) was added to a methanolic solution of morin (10 mL, 0.5 mmol). The pH value of the solution was adjusted to 5 by addition of a sodium methoxide ($NaOCH_3$) solution. After refluxing for 3 h, a green brownish solid was formed. The hot resulting suspension was filtered, washed three times with methanol and dried in an oven at 60 °C. (Found: C, 46.2; H, 3.9; V, 6.3. $C_{30}H_{30}O_{21}V$ requires C, 46.3; H, 3.9; V, 6.5). UV–vis data for 1:2 $V(IV)O^{2+}$ to morin ratio, pH 5, λ_{max} (DMSO) 560 nm (sh) (ε, 118 M^{-1} cm^{-1}, $3d_{xy} \rightarrow 3d_{x2-y2}$), 753 nm (ε, 33 $M^{-1}.cm^{-1}$, $3d_{xy} \rightarrow 3d_{xz}$, $3d_{yz}$). Thermal analysis (TGA) (oxygen atmosphere, velocity, 50 mL min^{-1}): in a first step (20–100 °C) the five water hydration molecules are lost (Δw_{calc}. 11.54%, Δw_{found} 11.94%) with an endothermic DTA signal). The coordinated water molecule is lost at higher temperature, as expected, together with the initiation of ligand decomposition. The final residue up to 900 °C was characterized by infrared spectroscopy as V_2O_5. The weight of the final residue was in agreement with the theoretical value (11.71%). Diffuse reflectance spectrum: λ_{max} 630 nm, >800 nm.

2.4. Spectrophotometric titrations

In order to establish the stoichiometry of the complex the molar ratio method was applied. A methanolic solution of morin (4×10^{-5} M) was prepared and its electronic spectrum recorded. The absorption spectra of different methanolic solutions of 4×10^{-5} M morin and $VOSO_4 \cdot 5H_2O$ in ligand-to-metal molar ratios from 10 to 0.5 (pH 5) were measured.

2.5. Antioxidant properties

The antioxidant assays (superoxide dismutase (SOD) activity, antiradical 1,1-diphenyl-2-picrylhydrazyl radical (DPPH·), 2,2′-azinobis(3-ethylbenzothiazoline-6-sulfonic acid) diammonium salt decoloration assay, scavenging of the hydroxyl radical and the inhibition of peroxyl radical) were performed according to our previously reported techniques [15]. In these experiments morin and VOmor complex were dissolved in the minimum quantity of DMSO and they were added to the aqueous buffer and the substrate solutions. The same quantity of DMSO was added to the solutions for the basal state measurements in each case.

2.6. Cell culture

MC3T3E1 osteoblastic mouse calvarium-derived cells and UMR106 rat osteosarcoma-derived cells were grown in DMEM supplemented with 100 U/mL penicillin, 100 μg/mL streptomycin, and 10% (v/v) FBS at 37 °C, 5% CO_2. When 70–80% confluence was reached, cells were sub-cultured using 0.1% trypsin 1 mM EDTA in Ca(II)–Mg(II)-free phosphate-buffered saline (PBS) (11 mM KH_2PO_4, 26 mM Na_2HPO_4, 115 mM NaCl, pH 7.4). For experiments, cells were grown in multiwell plates. When cells reached 70% confluence, the monolayers were washed twice with DMEM and were incubated in different conditions depending on the experiments.

Human T47D and SKBR3 breast cancer cell lines were obtained from HPA Culture Collection (Salisbury, United Kingdom). The T47D cell line was cultured in endotoxin-free RPMI medium supplemented with 10% FBS, 1% non-essential amino acids and 100 U/mL penicillin and 100 μg/mL streptomycin. SKBR3 cells were cultured in endotoxin-free Mc Coy medium supplemented with 10% FBS and 100 U/mL penicillin and 100 μg/mL streptomycin. All reagents were from Sigma–Aldrich (St. Louis, MO). Primary human mammary epithelial cells were obtained from ScienCell Research Laboratories and were grown in mammary epithelial medium media supplemented with 1% mammary epithelial growth supplement and 100 U/mL penicillin and 100 μg/mL streptomycin. Cultures were maintained at 37 °C in a humidified atmosphere with 5% CO_2 and passaged according to manufacturers' instructions.

2.7. Biological assays

Cell proliferation, and cell morphology experiments were performed with $V(IV)O^{2+}$, VOmor, and the free ligand. Intracellular formation of reactive oxygen species (ROS) was also determined. Briefly, the cell proliferation of the osteoblasts was assessed by the crystal violet bioassay. Stock complex solutions were prepared by dissolving VOmor in hot DMSO with a manipulation time of 15 min. Then, the solution of the complex was immediately diluted with DMEM. The maximum concentration of DMSO in DMEM was always lower than 0.5%, being innocuous for the cultures. Then, the complex solution was added to the cells in different concentrations and the cells were incubated for 24 h. The cells in culture were stained with crystal violet after the incubation period. Next, they were washed to remove the excess of dye. The crystal violet taken up by the osteoblasts was extracted with the appropriate buffer and the absorbance was measured at 540 nm. Previously, a linear correlation was established for the number of cells and the absorbance [16].

Breast cancer cells T47D and SKBR3 and primary human mammary epithelial cells were seeded at a density of 5000 cells/well in 96 well plates, grown overnight and treated with either vehicle, morin, VOmor and oxovanadium(IV) of different concentrations in FBS free medium. The dissolution vehicle was DMSO to yield a maximum final concentration of 0.5% in the treated well (Sigma–Aldrich, St. Louis, MO). After 24 h of incubation, 3-(4,5-methylthiazol-2-yl)-2,5diphenyl-tetrazolium bromide (MTT) was added at 100 μg/well for 2 h (Sigma–Aldrich, St. Louis, MO). The formazan products generated by cellular reduction of MTT were dissolved in DMSO and the optical density was measured at 450 nm using Sinergy 2 Multi Mode Microplater reader Biotek (Wisnooski, USA). All experiments were done in triplicate. To examine cell viability together with nuclear morphology 4′,6′-diamidino-2-phenylindole (DAPI) probe was added in another experiment instead of MTT. A high-content imaging system was used. Briefly, the cell monolayers were washed twice, each time with 200 μL PBS. Then they were fixed with 4% paraformaldehyde solution and incubated for 5 min at room temperature. The formalin solution was aspirated and the cells were washed three times for 10 min each with 200 μL PBS at room temperature. The final PBS was aspirated, washed and 12 μM DAPI was added to each well incubating during 10 min at room temperature with and without (control) the added compounds. The DAPI solution was aspirated and the samples were washed three times with 200 μL PBS and then 100 μL PBS was added to each well. The samples were analyzed by fluorescence microscopy using 350-nm excitation and 486-nm emission wavelengths.

The intracellular ROS generation in osteoblast-like cells was measured by oxidation of DHR123 to rhodamine 123. Osteoblast-like cells were incubated during 30 min at 37 °C in 1.5 mL of Hank's Buffered Salt Solution (HBSS) alone (basal condition) or with morin, VOmor and $V(IV)O^{2+}$, in the presence of 10 mM DHR123 [17]. Media were separated and the cell monolayers rinsed with PBS and lysated into 1 mL 0.1% Triton-X100. The cell extracts were then analyzed for the oxidized product rhodamine123 by measuring fluorescence (excitation wavelength, 500 nm; emission wavelength, 536 nm), using a Perkin–Elmer LS 50B spectrofluorometer. Results were corrected for protein content, which was assessed by the method of Bradford [18].

The morphology of the osteoblasts was then determined. They were grown in six-well plates and incubated overnight with fresh serum-free DMEM plus 0 (basal) and 10 μM solutions of the complex. The monolayers were subsequently washed twice with PBS, fixed with methanol, and stained with 1:10 dilution of Giemsa stain for 10 min [19]. Next they were washed with water and the morphological changes were examined by light microscopy.

For the high content analysis image assay the T47D and SKBR3 cells were seeded at a density of 5000 cells/well in a collagen-coated 96 well plate and stained with fluorescent probes (Invitrogen, Life Technologies, Madrid, Spain) during 30 min: tetramethyl rhodamine methyl ester (TMRM) 50 μM for the measurement of mitochondrial depolarization related to cytosolic Ca^{2+} transients, 5-(and-6)-chloromethyl-2,7,dichlorodihydrofluorescein diacetate acetyl ester (CM-H2DCFDA) 1 μM for the determination of reactive oxygen species production (ROS) and CellEvent™ Caspase 3/7 Green Detection Reagent 5 μM for the assessment of caspase 3/7 activation. After 30 min cells were treated with 10 μM concentration of morin, VOmor and oxovanadium(IV) during 24 h. Some cells received 100 μM H_2O_2 as positive control for ROS and TMRM measurement and 10 μM staurosporine as positive control for Caspase 3/7 activation. Image acquisition was performed using a Becton

Dickinson Pathway plate imager with a 10x Olympus Objective. The excitation/emission filters for each probe were: 488/10 nm and 515LP nm (ROS), 555/28 nm and 647/78 nm (TMRM), 488/10 nm and 515LP nm (CellEvent™ Caspase 3/7 Green Detection Reagent). Using specific AttoVision (BD) software algorithms, the mean intensity of each Region of Interest (ROI) was analyzed.

After the measurements with the probes, conditioned medium from each well was collected for LDH assay. This assay was performed according to the manufacturer's protocol. LDH release to the culture medium was determined using a Sinergy 2 Multi Mode Microplater reader Biotek (Wisnooski, USA) at 340 nm.

To detect DNA damage cells were fixed with 3% paraformaldehyde for 30 min at room temperature and permeabilized with 0.3% triton for 10 min. Cells were blocked during 30 min with 3% BSA in PBS. Then they were incubated with 2 μg/mL mouse monoclonal H2AX (Abcam, Cambridge, United Kingdom) for 1 h at room temperature. The secondary antibody used was Alexa 633 goat antimouse. Images were acquired on a BD Pathway™ Bioimager (Becton Dickinson).

At least three independent experiments were performed for each experimental condition in all the biological assays. The results are expressed as the mean ± standard error of the mean.

3. Results and discussion

3.1. Solid characterization of the complex

3.1.1. Infrared spectra

The Infrared spectra have been used to validate the proposed structure of the complex. Table 1 shows the position of the most important FTIR bands of morin and its complex with oxovanadium(IV). The FTIR spectra of the ligand and VOmor were recorded in the 4000–400 cm^{-1} region. The comparison of both spectra revealed important spectral changes. The characteristic band of carbonyl group ν(C=O) in morin appeared at 1661 cm^{-1}, while in the complex it appeared at 1637 cm^{-1}. The shift of 24 cm^{-1} to lower wavenumbers due to the increase of the C=O bond length suggested that the ligand coordination took place through the oxygen atom of the carbonyl group. Besides, the bands associated with the vibrational deformation modes of the OH groups reduced their intensities or changed upon deprotonation and/or coordination to the oxovanadium(IV) ion. New bands at 1550 cm^{-1} and 1420 cm^{-1} were related to the antisymmetric and symmetric C–O stretching modes at the chelating site [20]. In the VOmor spectrum the bands at 1550 cm^{-1} were overlapped while the symmetric C–O mode was observed as a shoulder at 1424 cm^{-1}. These results suggested that metal coordination most probably occurred via carbonyl oxygen and OH groups (3- or 5-) of morin at the chelating site level. Similar wavenumber shifts had been shown for the VOquercetin complex [21]. However, the pattern of the electronic spectrum indicated that the OH group involved in the coordination site is the 3-OH moiety (see below). The band assigned to the stretching mode (ν(C=C)) did not show a considerable change by complexation indicating insignificant structural changes of the two rings. The band (ν(COC)) was slightly shifted indicating a weak alteration of the ring structure and lack of interaction of the oxygen atom of the ring with the metal atom [22]. The O–H stretching bands of VOmor that appeared as broad bands in the (3700–3000 cm^{-1}) range were also been assigned to the water molecules of crystallization [23]. The broad stretching band observed at 973 cm^{-1}, characteristic of the V=O stretching, appeared in the typical range reported in the literature for oxovanadium(IV) species and its position indicated that there is no intermolecular interaction with participation of the V=O moiety.

Table 1
Tentative assignments of the main bands of the infrared spectra of Morin and the oxovanadium(IV) complex, VOmor (band positions in reciprocal centimeters).

Assignments	Morin	$[VO(mor)_2H_2O].5H_2O$
ν(OH)	3371 br, 3142 br	3411 br
ν(C=O)	1661 m	1637 sh
$\nu(C{=}C)_{aromatic\ ring}$	1624 vs	1618 vs
$\nu(C{=}C)_{aromatic\ ring}$ + $\nu(C{-}O)_{as}$ + δ(5OH) + δ(7OH)	1612 sh	1594 sh
δ_{ip}(CH)	1509 s	1510 m
δ_{ip}(C8H) + δ(7OH)	1460 s	1457 m
$\delta(C{-}O)_s$		1424 sh
δ(C–OH)	1382m	1357 vw
δ(C–O–C)	1252 w	1271 sh
δ_{ip}(C3H), δ(5OH), (7OH)	1228 w	1229 sh
Ring B, δ_{ip}(CH)	1172 vs	1173 w
δ_{ip}(COC), δ_{ip}(CH)	1102 vw, 1085 sh	1108 w
δ_{ip}(CH)	1010 w, 973 w	
ν(V=O)		979 br
δ(C–H)	971 m	

vs, very strong; s, strong; m, medium; w, weak; sh, shoulder; δ_{ip}, in-plane bending; br, broad.

3.1.2. EPR spectroscopy

The EPR spectrum of the VOmor was measured at room temperature and gave an eight-line hyperfine splitting pattern due to the unpaired electron of the ^{51}V nucleus ($I = 7/2$) being indicative of the presence of only one mononuclear oxovanadium(IV) species in the solid complex. The experimental spectrum can be simulated using the calculated parameters and the fitted spectrum was in agreement with the experimental one (Fig. 2a).

The simulation (Fig. 2b) predicted that the observed signal originated from a vanadium chromophore was consistent with the oxovanadium(IV) ion in a nearly axial or pseudoaxial ligand field. The spin Hamiltonian parameters and the hyperfine coupling constants were $g_{II} = 1.942$; $A_{II} = 172 \times 10^{-4}\ cm^{-1}$; $g_{\perp} = 1.976$; $A_{\perp} = 67 \times 10^{-4}\ cm^{-1}$ ($g_{iso} = 1.965$, $A_{iso} = 102 \times 10^{-4}\ cm^{-1}$). The additivity relationship for oxovanadium(IV) complexes, $A_z = \Sigma n_i A_{z,i}$, concerning the magnitude of A_z introduced by Chasteen [24], can provide the identity of the equatorial donor sets coordinated to $V(IV)O^{2+}$ entity. In this formula, n_i is the number of equatorial ligands of type i and $A_{z,i}$ is the contribution to the parallel hyperfine

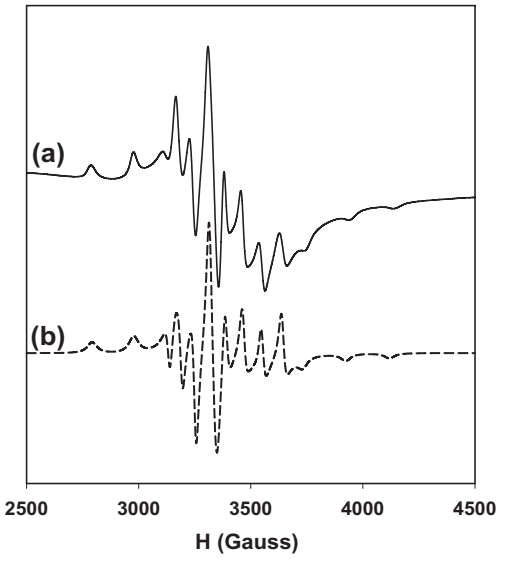

Fig. 2. Experimental (a) and calculated (b) powder EPR spectra of $[VO(mor)_2H_2O]{\cdot}5H_2O$ measured at X-band (9.4006 GHz, 290 K).

coupling of the most probable metal center coordination environment. Each donor group had a specific contribution to this constant and the sum of the contributions of the four equatorial ligands can be compared with the observed value. Taking into account the probable and expected donor set, the calculated A_z value of 173.7 $\times 10^{-4}$ cm^{-1} (considering two C=O, one ArO$^-$ and one water molecule) was obtained bearing in mind the literature values for the contribution of each donor group to A_z = ArO$^-$, 38.6 $\times 10^{-4}$ cm^{-1}; C=O, 44.7 $\times 10^{-4}$ cm^{-1} and H_2O, 45.7 $\times 10^{-4}$ cm^{-1} [21,25]. This calculated A_z value corresponded well with the experimental one, suggesting that the binding mode of this complex could be expected to involve an equatorial coordination sphere with two oxygen atoms from C=O groups, one deprotonated ArO$^-$ (from the flavonoid moiety of the ligand), one water molecule bounded to the oxovanadium (IV) center, giving the well known *cis*-$VOL_2{\cdot}H_2O$ structure in maltol-type compounds [25].

3.2. Solution studies

3.2.1. Electronic spectra

In order to confirm the presence of the different protonated forms of morin at different pH values the UV–vis spectra of the flavonoid were recorded using methanolic solutions. The spectral changes can be seen at pH 5, pH 9 and at pH 10 (Fig. 3) in agreement with the previous reports [26].

To determine the pH at which the interaction of the ligand with the metal center started, measurements of the electronic spectra of methanolic solutions of morin:VO, in a 2:1 ligand-to-metal ratio, at different pH values were carried out (Fig. 4). At pH above 5, the band located at 422 nm widens, indicating that there is a change in the electronic levels of the flavonoid. Thus, we can assume that the interaction of the ligand with the metal center begin at this pH value.

From the spectra of flavonoid metal complexes, significant information about the coordination sites can be obtained, if the different electronic absorption spectra of the ligands at different pH values are taken into consideration. The spectrum of VOmor shows a shift toward the red, as compared to the spectrum of morin (Fig. 5). This bathochromic shift in both absorption bands of the ligand is typical for complex formation.

With the aim to confirm the stoichiometry of the complex VOmor spectrophotometric titrations were performed. Fixing the pH value at 5 and starting at a ligand-to-metal ratio of 10:1, the band at 422 nm increased upon addition of different quantities of V(IV)O^{2+} (Fig. 6). The molar ratio plot indicated the formation of a 2:1 morin:VO complex (Fig. 6, inset).

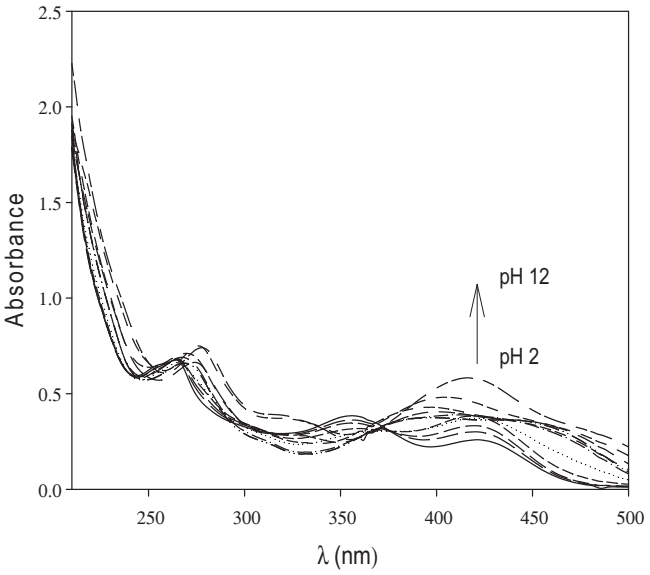

Fig. 4. Spectra of $VOSO_4{\cdot}5H_2O$ (2×10^{-5} M) and morin (4×10^{-5} M), methanolic solutions, at different pH values.

3.2.2. Solution EPR spectra

In order to assist in the identification of the different vanadium species, the spectrophotometric titrations were followed by EPR spectroscopy. In Fig. 7 (left) the EPR spectra (X-band, 150 K) at various M:L metal-to-ligand ratios (pH 5, ethanol) are shown. In this experiment, vanadyl sulfate pentahydrate was used to obtain V(IV)O^{2+} cation in solution, able to interact with morin.

As it is depicted in Fig. 7, from metal-to-ligand ratios of 1:10 up to 1:2 (a–d in Fig. 7, left) only one EPR signal can be observed indicating the formation of single species (I) in this concentration range. The spectral simulation predicted the formation of a V chromophore with the spin Hamiltonian parameters and the hyperfine

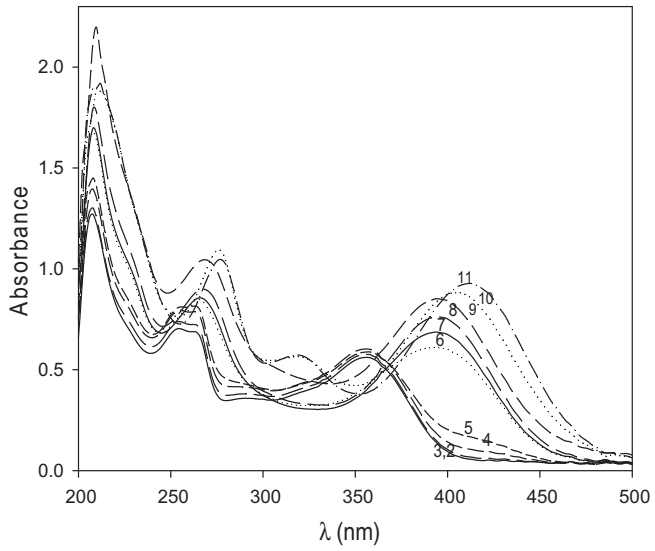

Fig. 3. Spectra of morin (4×10^{-5} M), methanolic solutions, for different pH values (in arabic numbers).

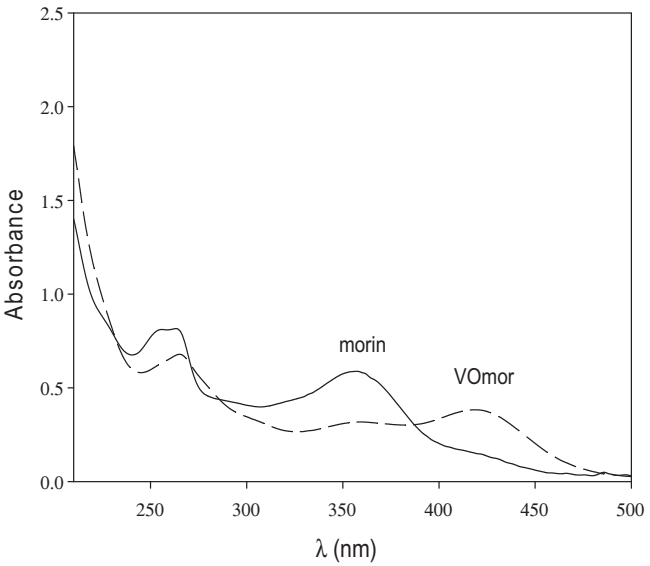

Fig. 5. UV–visible spectra of the ligand morin and the complex VOmor in methanol.

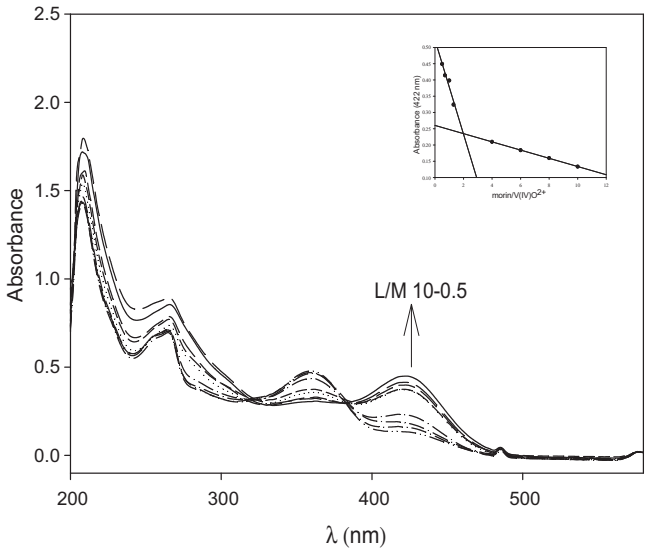

Fig. 6. UV–visible spectra of morin (4×10^{-5} M) with the addition of $VOSO_4 \cdot 5H_2O$ in ligand-to-metal ratios (L/M) from 10.0 to 0.5 (pH 5). The arrow indicates increasing metal additions. Inset: Spectrophotometric determination of VOmor complex stoichiometry at λ_{max}/nm 422 by the molar ratio method.

coupling constants of $g_{II} = 1.937$; $A_{II} = 174.5 \times 10^{-4}$ cm^{-1}; $g_{\perp} = 1.980$; $A_{\perp} = 65 \times 10^{-4}$ cm^{-1}. For metal-to-ligand ratios higher than 0.5 (e–h in Fig. 7, left), considerable modification in the EPR spectra was detected and two different signals were observed: species I and a new species indicated as II. Applying the formula described above ($A_z = \Sigma n_i A_{z,i}$) it has been found that for the species I the calculated parameters were in the usual range found for oxovanadium(IV) compounds with O4 coordination sphere. Considering the different contributions to the parallel hyperfine coupling constant (see above) and taking into account that there are no large differences in the hyperfine coupling constant values between water and ethanol [27], we conclude that the conformation of species I would correspond to a similar binding mode like the solid complex with an equatorial donor set of 2(C=O), 1(Ar–O$^-$) and one ethanol (solvent) molecule in the fourth position of the equatorial plane (*cis*-$VOL_2 \cdot$EtOH). These results are in accordance with that obtained in the spectrophotometric titration measurements suggesting the formation of VOL_2 as the main species in solution at pH 5. The signal of species II was also simulated (Fig. 7, right) and the calculated Hamiltonian parameters and hyperfine coupling constant correlated well with those of $V(IV)O^{2+}$ cation measured in ethanolic solution ($g_{II} = 1.933$; $A_{II} = 181.5 \times 10^{-4}$ cm^{-1}; $g_{\perp} = 1.979$; $A_{\perp} = 70.5 \times 10^{-4}$ cm^{-1}).

3.3. Antioxidant properties

The superoxide scavenger activity was determined measuring the SOD mimetic actions of the ligand and the complex (Fig. 8 and Table 2). The concentration of morin that produced a 50% inhibition of the reduction of NBT by the superoxide anion (IC_{50}) was 66 μM.

This value was different from other values reported previously because of the different sources of superoxide radical generation used. For VOmor the calculated IC_{50} value of 54 μM showed that the superoxide scavenging capacity was slightly improved by complexation. However, this complex does not seem to be a SOD mimetic agent because this value is nearly three times greater than the value required to be considered a good SOD mimic (20 μM). In addition, earlier reported IC_{50} values for native enzyme and oxovanadium(IV) cation under our experimental determinations were 0.21 μM and 15 μM, respectively [28].

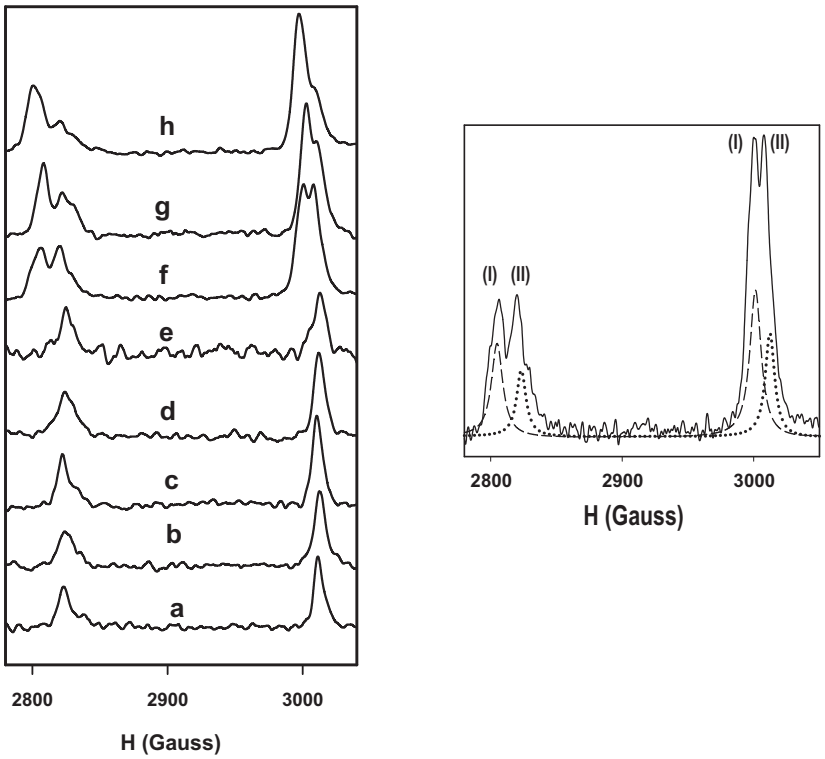

Fig. 7. Low-magnetic field parallel region of the EPR spectra recorded at 150 K in ethanolic solutions of the $V(IV)O^{2+}$ and morin system. Left: (a = 1:10, b = 1:7, c = 1:4, d = 1:2, e = 1:1.5, f = 1:1, g = 1:0.7, h = 1:0.5). Right: solid line, M:L = 1:1; dashed line, simulated specie II (ethanol) $V(IV)O^{2+}$, oxovanadium(IV) solution (1×10^{-3} M); dotted line, simulated species I (*cis*-$VOL_2 \cdot$EtOH). Total Morin concentration: 1×10^{-3} M.

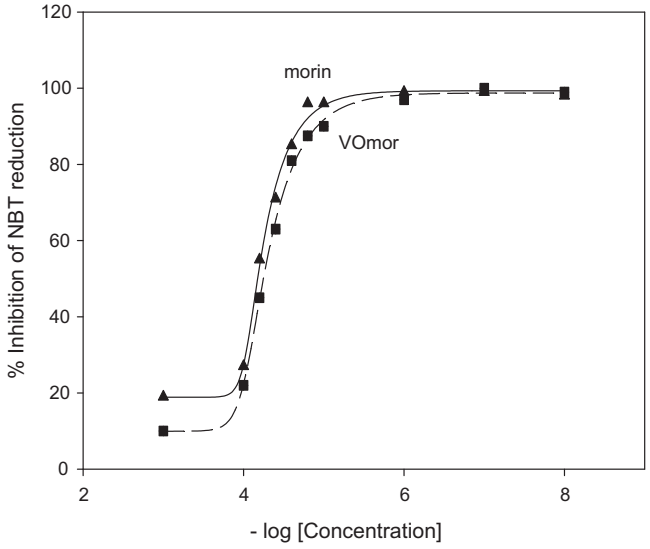

Fig. 8. Effects of morin and VOmor on the reduction of nitroblue tetrazolium by the generated superoxide (phenazine methosulfate and reduced nicotinamide adenine dinucleotide system). The system contained sample, NADH (1.40 mM) and NBT (300 μM), in phosphate buffer (pH 7.5). After incubation at 25 °C for 15 min, the reaction was started by adding PMS (120 μM). Then, the reaction mixture was incubated for 5 min and the absorbance at 560 nm was measured.

Table 2
Percentage of free radical scavenging of morin, VOmor and oxovanadium(IV). Values are expressed as the mean ± standard error of at least three independent experiments.

Radical	% scavenging		
	Morin	VOmor	$V(IV)O^{2+}$
SOD (IC_{50}, μM)	66	54	15
$DPPH^{\cdot}$, 10 μM	15.0 ± 0.7	22.0 ± 1.0	2.0 ± 0.3
$ABTS^{+\cdot}$, 10 μM	76.0 ± 0.5	81.0 ± 1.5	4.0 ± 0.3
TEAC[a]	2.05	1.98	0.2
$OH^{\cdot}$, 10 μM	1.7 ± 0.9	25.7 ± 1.8	3.0 ± 0.5

[a] Trolox equivalent antioxidant activity.

Both the free ligand and the complex VOmor showed a similar DPPH radical scavenger capacity. As shown in Table 2 at 10 μM concentrations they have an intermediate ability to scavenge $DPPH^{\cdot}$ radicals (15% and 22%, respectively).

The ABTS assay allows the determination of the total antioxidant activity (TAA) and the Trolox equivalent antioxidant activity (TEAC) measuring the concentration of a Trolox solution with an equivalent antioxidant potential to a standard concentration of the compound under investigation. Our measurements indicate a great antioxidant activity for morin and VOmor. The obtained TEAC values were 2.05 (morin) and 1.98 (VOmor). It can be seen that the complexation does not improve the antioxidant activity (Table 2).

Deoxyribose is attacked by hydroxyl radicals ($OH^{\cdot}$) to form a product that reacts on heating with thiobarbituric acid (TBA) developing a pink chromogen (λ = 532 nm). Hydroxyl radicals were generated by a mixture of Fe^{3+}, ascorbic acid and H_2O_2 in the presence of a slight excess of EDTA over the iron salt [29]. In Table 2 the effect of 10 μM VOmor and morin is depicted. The results clearly demonstrated that the antioxidant activity of the complex against $OH^{\cdot}$ (26% of degradation of the radical at 10 μM) was significantly higher than that of the ligand. It was then confirmed that morin did not show significant $OH^{\cdot}$ radical scavenging capacity in accordance with previous studies [30] and that the binding of the 3-OH group to the metal center improved the degradation power.

Pyranine is a spectrophotometric probe that scavenges free radicals, including AAPH-generated peroxyl ($ROO^{\cdot}$) radicals. The reduction in pyranine intensity is followed at 454 nm to monitor its interaction with peroxyl radicals. Pyranine declines at a constant rate with minimum delay (lag) following the addition of AAPH. In Fig. 9 it is observed that the lag phase increases with morin concentration, but is almost constant with increasing complex concentration. This indicates that VOmor is not an effective $ROO^{\cdot}$ radical scavenger.

3.4. Osteoblastic cells

3.4.1. Cell proliferation

The results of cell proliferation on two osteoblast-like cell lines in culture: UMR106 derived from a rat osteosarcoma and MC3T3E1 from mouse calvaria for different concentrations of VOmor, morin and the oxovanadium(IV) cation is shown in Fig. 10.

The effects of 10 μM solutions of the compounds on these cell lines are displayed in Table 3. The results show that the three compounds display inhibition of the proliferation of the MC3T3E1 cell line and that VOmor behaves as a more deleterious agent (26% inhibition at 10 μM).

As it has previously shown, the oxovanadium(IV) cation has no cytotoxic effect on the UMR106 proliferation [16]. A proliferative effect is observed in the UMR106 cell line for VOmor up to 50 μM and the behavior of morin is similar to the basal state. These results indicate that the complexation do not improve the antiosteosarcoma activity.

3.4.2. Intracellular ROS generation

While the biochemical mechanism of vanadium carcinogenicity and toxicity is still not fully understood, some studies have indicated that vanadium-mediated generation of related oxygen species may play an important role [31]. In this context, ROS production by morin, $V(IV)O^{2+}$ cation and VOmor in UMR106 line cell and MC3T3E1 line cell has been measured herein. The DHR probe has great affinity for the mitochondria and is oxidized to the fluorescent agent rhodamine 123 in the presence of oxidant agents. As mentioned earlier, the probe used in this assay can detect different ROS, particularly H_2O_2 [32]. As shown in Table 3, both 10 μM morin and VOmor deplete the ROS level, but the $V(IV)O^{2+}$ cation stimulate the generation of ROS in the non-transformed osteoblasts. Neither of 10 μM morin, VOmor and $V(IV)O^{2+}$ produce

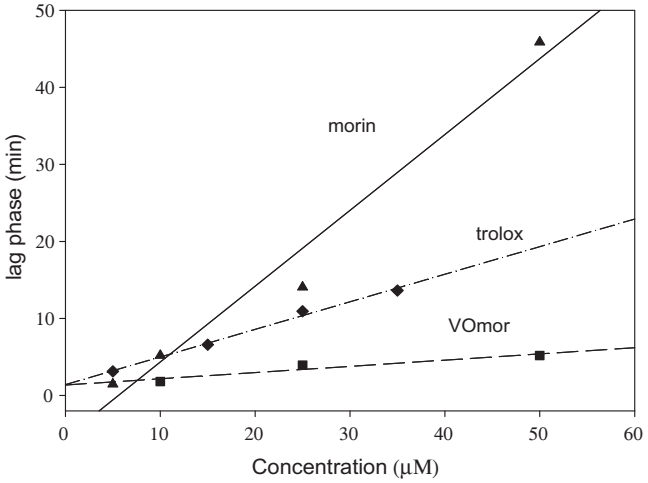

Fig. 9. Effect of trolox, morin, VOmor on AAPH-generated peroxyl radicals pyranine mixture. Changes were calculated as time delay (lag) of pyranine consumption. The reaction solutions contained AAPH (50 mM), pyranine (50 μM) and several concentrations of the tested compounds. The consumption of pyranine (37 °C) was followed spectrophotometrically by the decrease in absorbance at 454 nm.

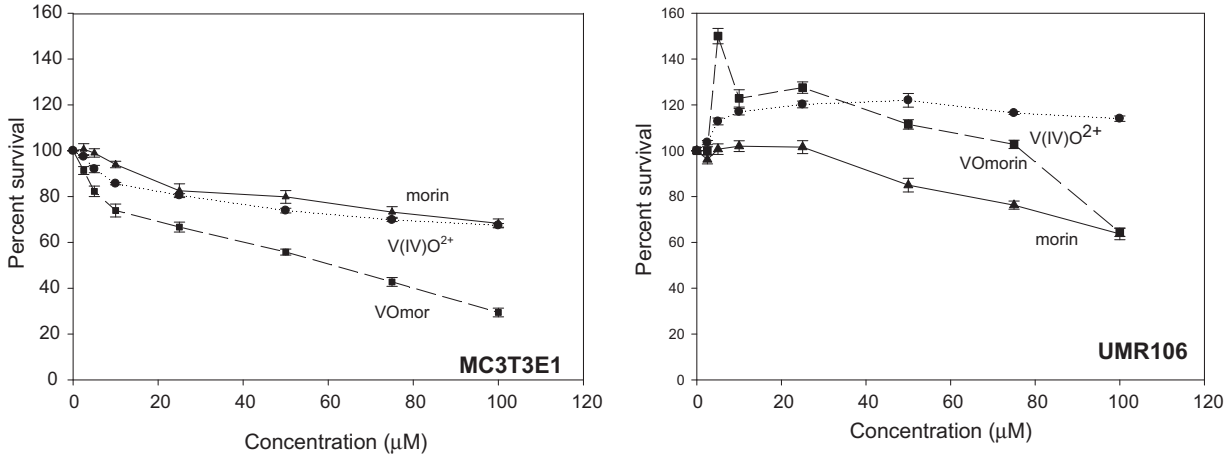

Fig. 10. Effects of morin, VOmor and $V(IV)O^{2+}$ on MC3T3E1 and UMR106 cell proliferation. Cells were incubated in serum-free Dulbecco's modified Eagle's medium (DMEM) alone (basal) or with different concentrations of the compounds at 37 °C for 24 h. The results are expressed as the percentage of the basal level and represent the mean ± standard error of the mean (SEM).

Table 3
Effects of morin, VOmor and $V(IV)O^{2+}$ on osteoblast-like cells. Proliferation: Cells were incubated in serum-free Dulbecco's modified Eagle's medium (DMEM) alone (basal) or with 10 μM of the compounds at 37 °C for 24 h. ROS production: DHR 123 oxidation to rhodamine 123, cells were incubated alone (basal) or with 10 μM of the compounds at 37 °C in the presence of 10 mM DHR 123. The results are expressed as the percentage of the basal level and represent the mean ± SEM ($n = 9$).

	Proliferation (% basal)			ROS production (% basal)		
	Morin	VOmor	$V(IV)O^{2+}$	Morin	VOmor	$V(IV)O^{2+}$
MC3T3E1	94.0 ± 1.4	73.9 ± 2.8	85.7 ± 0.5	22.1 ± 1.7	74.1 ± 7.9	232.4 ± 8.1
UMR106	101.9 ± 2.3	122.8 ± 3.8	117.0 ± 1.4	104.7 ± 15.9	81.6 ± 7.8	88.4 ± 8.8

significant quantities of ROS in the UMR106 cell line (Table 3). Summarizing, the effect observed in the cells is in agreement with the antioxidant effect observed in *in vitro* experiments in which VOmor behaves as a hydroxyl radical scavenger and morin as a peroxyl sequestering agent.

3.4.3. Cell morphology

The normal MC3T3E1 osteoblastic cells under basal conditions (without any compound added) show polyhedral morphology with thin lamellar expansions that allow cells to attach to each other (Fig. 11a).

Their nuclei have rounded shape and chromatin granules and nucleoles are detected. After incubation with VOmor (10 μM) a decrease in cell number and a condensation of the cytoplasm (58% determined with the processor images program ImageJ) with the presence of bubbles are observed. The nucleus retains their morphology. On the other hand, the tumoral cells, both at basal conditions and at 10 μM concentrations, polygonal morphology cells with nuclei of different shapes and sizes are observed (Fig. 11b). The presence of nucleoles can also be seen. The cells have several connections between them.

3.5. Human breast cells

3.5.1. Cell viability assay (MTT method)

Taking into account the non-specificity found for morin and VOmor for the treatment of osteosarcoma, we have investigated the breast tumor cells in order to determine the sensitivity of these compounds for breast cancer and to achieve a deleterious effect on breast cancer before the production of bone metastasis. The non-tumorigenic breast epithelial mammal cells were selected as the normal cell line and are not affected by the addition of morin and VOmor (Fig. 12). Besides, from the experimental data (Table 4

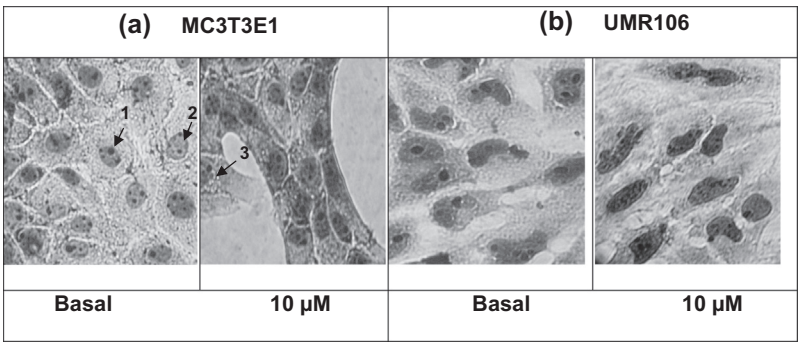

Fig. 11. Effect on cell morphology of the treatment of the osteoblast-like cells with VOmor (10 μM) in comparison with basal or control conditions (without any compound added). (a) MC3T3E1 non transformed osteoblast cells; (b) UMR106 osteosarcoma cells. (Arrows indicated: (1) nucleoles, (2) chromatin granules, (3) cytoplasmic bubbles).

and Fig. 12) it can be seen that an improvement of the antitumoral effect upon complexation on the T47D and SKBR3 lines is achieved.

In addition, the cell-permeable nucleic acid stain 4′,6′-diamidino-2-phenylindole (DAPI) was also added to assess nuclear morphology by fluorescence microscopy. The microscopic observations on the nuclear cancer cell morphology revealed that VOmor treatment induced a noticeable reduction in the nuclear size (see Fig. 13).

3.5.2. Mechanisms of the effect of VOmor in the T47D and SKBR3 cell lines

It was shown above that a 10 μM solution of VOmor produces a deleterious effect of ca. 40% in both cell lines. In order to understand the mechanisms of action of the compounds, in the course of the induction of cell death, we have investigated the effects of morin and its oxovanadium(IV) complex on intracellular ROS formation, mitochondrial membrane potential disruption, caspase 3/7 activation, nuclear damage and LDH release. The cells were treated with 10 μM concentration of complex, flavonoid or $V(IV)O^{2+}$ for 24 h. The effect of the compounds on the different studied parameters is displayed in Table 5. Fig. 13 shows a control group with cells showing 30–40% confluence with a vast majority of cells maintaining viability and normal mitochondrial characterization.

To evaluate whether the oxidative stress in the tested breast cancer cells is increased during the treatment with the compounds, we incubated the cells with CM-H2DCFDA probe. Results show that the three compounds do not generate significant enhancement in cell fluorescence due to intracellular ROS production. As expected, an important increase in cell oxidative stress is measured when 100 μM H_2O_2 was used as an internal control (data not shown).

The effect of the compounds on the mitochondrial membrane potential (MMP) has been determined treating the cancer cells with the compounds and incubating them with TMRM. The ligand and the complex reduce MMP in the SKBR3 cell line by 20% and 46%, respectively (see Table 5 and Fig. 13). However, only VOmor displays an important effect on mitochondrial depolarization (32%) in the T47D cell line. No appreciable changes in membrane integrity are observed for the cells treated only with the vehicle (control group). The majority of the cells maintain their viability and normal mitochondrial characteristics in this case. Then, the activation of Caspase 3/7 in the two cell lines has been investigated using the fluorescent specific substrate. From Table 5 and Fig. 13 it can be seen that VOmor and morin cause an increase of 185% and 43% of caspase 3/7 activity, respectively, during the treatment of the SKBR3 cells with the compounds. However, only VOmor increased the activity in T47D cells (167%).

Table 4
Effects of morin, VOmor and $V(IV)O^{2+}$ on human breast cells. T47D cells were cultured in endotoxin-free RPMI medium supplemented with 10% FBS, 1% non-essential amino acids and 100 U/ml penicillin and 100 μg/ml streptomycin. SKBR3 cells were cultured in endotoxin-free Mc Coy medium supplemented with 10% FBS and 100 U/ml penicillin and 100 μg/ml streptomycin. Cells were incubated alone (basal) or with 10 μM of the compounds at 37 °C for 24 h. The results are expressed as the percentage of the basal level and represent the mean ± SEM ($n = 9$).

	Proliferation (% basal)		
	Morin	VOmor	$V(IV)O^{2+}$
Breast epithelial cells	134.0 ± 7.3	116.8 ± 13.4	119.0 ± 6.5
T47D	101.4 ± 3.0	57.6 ± 2.8	92.5 ± 1.6
SKBR3	85.9 ± 3.7	62.7 ± 8.0	77.6 ± 2.0

To test whether the compounds cause nuclear damage treated and control cells are labeled with an antibody against phosphorylated histone H2AX which is a recognized marker for DNA damage. No DNA damage has been observed by inmunofluorescence upon the addition of the compounds in the two cell lines. The same protocol confirmed that staurosporine causes an increase in DNA damage (data not shown).

4. Discussion

4.1. Solution studies

The deprotonation of the hydroxyl moiety influences the intrinsic antioxidant potential of the flavonoids, because deprotonation generally enhances their antioxidant action [33]. Thus, the knowledge of their physicochemical parameters, such as the acid dissociation constant and the p*K*a, is important in order to predict their antioxidant capacity. In addition, the knowledge of the p*K*a values allows the determination of the precise species present in a biological medium being fundamental in bioclinical and pharmacological research studies. Morin is a flavonol sparingly soluble in water and its p*K*a values cannot directly be determined in aqueous solution. Herrero-Martínez et al. determined the p*K*a values of morin for different methanol/water mixtures. The three p*K*a values obtained at physiological ionic strength ($I = 0.15$ M) and 60% methanol were 5.095 ± 0.032, 8.484 ± 0.025 and 10.366 ± 0.032. The first ionization corresponds to the OH group in position 2′. This fact can be attributed to the stabilization of the anion by formation of an intramolecular hydrogen bond [34]. These spectral changes are shown in Fig 3.

For dihydroxylated flavones it was reported that the p*K*a values for 3-OH group is almost two units higher than that for 7-OH. However, it is known that there is a competition between protons

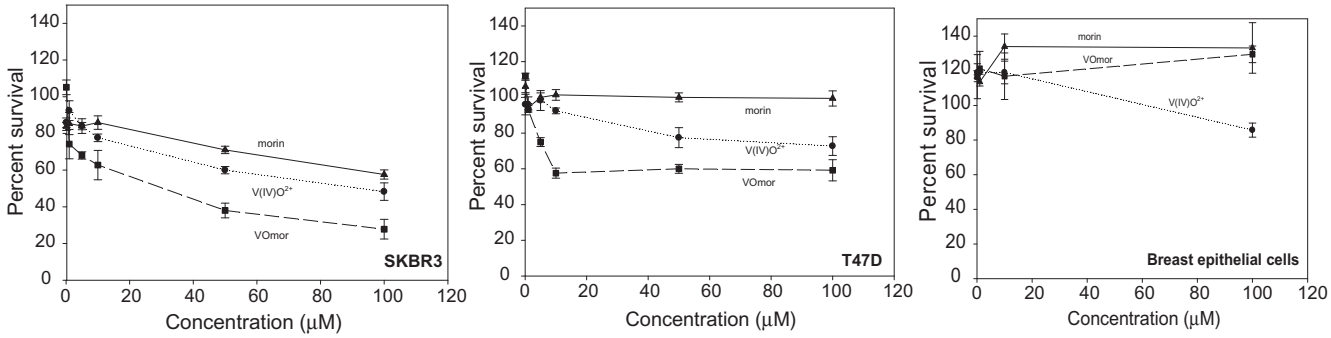

Fig. 12. Effects of morin, VOmor and $V(IV)O^{2+}$ on SKBR3, T47D and human breast epithelial cells viability. T47D cells were cultured in endotoxin-free RPMI medium. SKBR3 cells were cultured in endotoxin-free Mc Coy medium. Human breast epithelial cells were grown in mammary epithelial medium. Cells were incubated alone (basal) or different concentrations of compounds at 37 °C for 24 h. The results are expressed as the percentage of the basal level and represent the mean ± standard error of the mean (SEM).

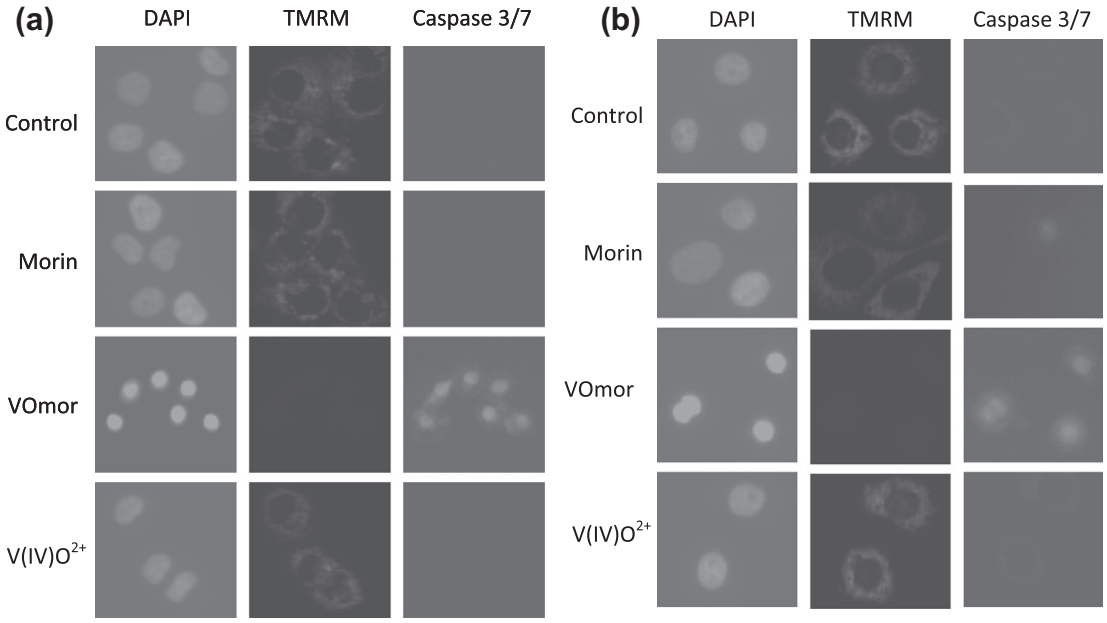

Fig. 13. (a) Mechanism of action of VOmor in T47D breast cancer cell line. Cells were treated with 25 μM of morin, VOmor and $V(IV)O^{2+}$ for 24 h. Then cells were incubated with DAPI, TMRM and caspase 3/7 activation fluorescent method for 30 min at 37 °C. (b) Mechanism of action of VOmor in SKBR3 breast cancer cell line. Cells were treated with 25 μM of morin, VOmor and $V(IV)O^{2+}$ for 24 h. Then cells were incubated with DAPI, TMRM and caspase 3/7 activation fluorescent method for 30 min at 37 °C.

Table 5
Effects of morin and VOmor on the viability and the possible mechanisms of action on SKBR3 and T47D human breast cell lines. High content analysis image assay: Reactive oxygen species, ROS were determined using the CM-H2DCFDA probe. Mitochondrial membrane potential disruption was detected using TMRM probe. Caspase 3/7 activation was determined using CellEvent™ Caspase 3/7 Green Detection Reagent. The measurement of LDH release (plasmatic membrane damage) was performed using the Cytotoxicity detection kit (LDH). Histone H2AX phosphorilation (DNA damage) was determined by an immunohistochemistry method.

	SKBR3		T47D	
	Morin	VOmor	Morin	VOmor
% survival	86%	62%	100%	57%
ROS	NO	NO	NO	NO
TMRM	Decrease (20%)	Decrease (46%)	NO	Decrease (32%)
CASP 3/7	Increase (43%)	Increase (185%)	NO	Increase (167%)
LDH	NO	Increase (126%)	NO	NO
H2AX	NO	NO	NO	NO

and metal ions for the conjugate base form of a ligand. Indeed, metal coordination of the hydroxyl group results in a substantial lowering of its p*K*a value because the inductive effect of a bound cation further polarizes the O–H bond [35]. Taking into account that the coordination of $V(IV)O^{2+}$ to the carbonyl oxygen atom and the 3-OH moieties generate a chelate ring and that the coordination at the 3-OH moiety can cause a reduction of the p*K*a value even lower than the p*K*a of the 7-OH moiety, we can conclude that among the 3- and the 5-OH groups the coordination of the metal center takes place through the 3-OH group.

The flavonoids display two major absorption bands in the UV–visible region. In the electronic absorption spectrum of morin in methanol there are two intense absorption bands; the band centered at 357 nm (band I) is due to the transition localized within the B ring of cinnamoyl system, whereas the one centered at 260 nm (band II) is consistent with absorbance of ring A of benzoyl system. They are related to π–π^* transitions [36]. Besides, the large shift ($\Delta\lambda$ = 66 nm) of band I (Fig. 5) have also been observed for other flavonoid metal complexes [19,20,25] and the new bands at ca. 430 nm were assigned to metal chelation through 3-hydroxychromone group. The origin of this band has been described by means of the electronic redistribution that occurred between the chelating ligand and the oxovanadium(IV) cation, forming a big extended π-bonding system and as a result, the electronic transition $n\pi^*$ of morin changes to π–π^* and appeared at lower energy. Considering the above data it is assumed that the coordination of morin to the metal center occurs through the carbonyl oxygen atom and the deprotonated hydroxyl group in 3-position and from the molar ratio plot (Fig. 6) a 2:1 ligand-to-metal stoichiometry (*cis*-VOL_2·EtOH, see Section 3.1.2) was achieved. Besides, the electronic spectrum of a 2:1 solution at pH 5 remained unaltered at least during 1 h (data not shown), indicating that the complex remained stable during the manipulations for the biological measurements.

4.2. Antioxidant behavior

In morin-related flavonols such as quercetin, fisetin and myricetin, the presence of a hydroxyl group at C-3′ in ring B and at C-3 in ring C is associated with a high superoxide scavenging activity (IC_{50} 1.63 ± 0.02, 1.84 ± 0.07 and 0.33 ± 0.03 μM, respectively, measured by the nitrite method) but in the case of morin and galangin the absence of free 3′-OH produced low superoxide scavenging activity (IC_{50} 9.1 ± 0.08 and 6.74 ± 0.32 μM, respectively) [37]. Under our experimental conditions the IC_{50} value determined for morin is similar to that of the VOmor complex.

The antioxidant activity of morin is associated to the appreciable contribution of the 3-hydroxy group on the C-ring, involved in H-atom transfer reaction to DPPH· to facilitate H-abstraction from the molecule by stabilizing the corresponding radical [38]. It was previously found, by means of experimental and computational methods, that 3-OH, 2′-OH and 4′-OH are the main reactive sites, as well as that the 3-O-2′-O quinone is the first product of the reaction, tending to prevail in the enol form through a tautomerism effect, whose observed structural arrangement corresponds to the 3-O semiquinone [39]. Our antioxidant (DPPH) measurements for morin are similar to other previously reported values (IC_{50} 17.89 μM [40] and 16.5 μM [41]). Upon complexation, the 3-OH group is involved in coordination to the vanadium atom and the 2′-OH and 4′-OH groups might probably take part during the H-abstraction.

The maximum effectiveness for cation radical $ABTS^{\cdot+}$ scavenging apparently requires the 3-OH group attached to the 2,3-double bond and adjacent to the 4-carbonyl in the C ring [42]. Otherwise, the highest activities among flavonols correspond to those with an *ortho*-dyhidroxy structure on B ring and a –OH group at position 3, like in quercetin. It has previously been reported that the arrangement of the two hydroxyl groups on the B ring, ortho (quercetin) versus meta (morin), did not influence the antioxidant activity, in contrast to an earlier report that found that quercetin had significantly higher radical $ABTS^{\cdot+}$ scavenging activity than morin [43]. Our data on morin agree with previous results (TEAC = 2.55 [42], 1.79 [44] and 1.20 [45]). The glycosylation of the hydroxy substituent on C-3 such as in rutin drops antioxidant activity, confirming the significance of this group [46]. But the coordination to the metal center enhances the resonance in ring C. While in the complex the fenolic 2′-OH and 4′-OH groups are not involved in metal interaction these groups may take part in the scavenging of the radical cation.

Quenching of hydroxyl radical by phenolic compounds is generally considered to undergo H-abstraction reaction and electron transfer process and the stability of the resulted phenoxyl radicals also significantly influence the reactivity of quenching hydroxyl radicals [47]. A 3′,4′-catechol structure in the B-ring strongly enhances the capacity to scavenge hydroxyl radicals facilitating electron delocalization by the generation of a stable *ortho*-semiquinone radical. Flavones lacking *ortho*-catechol structure (like morin) form relatively unstable radicals and are weak hydroxyl radical scavengers. Besides, substitution of 3-OH by a methyl or glycosyl group completely abolish the antioxidant activity of some flavonoids [48]. The improvement of the antioxidant capacity of morin upon complexation could probable be due to the participation of the deprotonated 3-OH group (and C4═O carbonyl group) in the chelation to the metal that might enhance electron delocalization of the odd electron of the ring C by π conjugation from the B-ring.

As expected, quercetin behaves as a better anti peroxyl radical agent than morin. At a 10 μM concentration, quercetin causes more delay in pyranine consumption by $ROO^{\cdot}$ (26.1 min vs. 5.2 min for morin) [49]. However, it can be seen in the Fig. 9 that 10 μM trolox (reference compound) is less effective in the removal of peroxyl radicals than morin. When the colored compound pyranine is incubated with AAPH in the presence of VOmor the measured lag phase (induction time) results lower than for morin. The slopes of the curves of induction time versus concentration indicate a higher reactivity of morin with AAPH-derived peroxyl radicals, inhibiting the free radical damage to pyranine, and a lower reactivity of VOmor toward the peroxyl radicals enhancing the pyranine oxidation.

In conclusion, it was observed that the complex showed higher suppression effect toward superoxide and hydroxyl radicals than that of morin indicating a higher ROS scavenging effect. However, the peroxyl radical scavenging activity of VOmor was lower than that of free morin.

4.3. Cancer cells

We have demonstrated in this work that VOmor is quite toxic to breast tumor cells exhibiting promising cytotoxicity with regard to (T47D and SKBR3) cancer cell lines. We investigated the factors which might be involved in the mechanism underlying the cytotoxic effects of the complex and compared this behavior with that of the parent drugs. We have also determined that the VOmorin complex did not exert antiosteosarcoma effects. Although VOmor has some deleterious behavior on the proliferation of the MC3T3E1 cells, the production of ROS is lower than in the basal state. Therefore, a probable mechanism involved in the deleterious action of the complex at concentrations of 10 μM may also be related to the effect of other free radicals that cannot be detected by the DHR 123 probe or to another apoptotic process. The cellular morphology of the bone cells is in agreement with the cytotoxic determinations.

The tumor-specific cytotoxicity behavior of some flavonoids was previously determined [50]. Those authors demonstrated that four of the tested tumor cell lines were more sensitive to the assayed flavonoids than the three normal cells assayed, and they calculate a tumor specificity index. But the tumor cell lines indeed, showed considerable variation in sensitivity between them. We have found that the VOmor and the parent drugs have no cytotoxic effects against normal breast epithelial mammal cells, and that VOmor show comparable cytotoxicity and tumor-specificity against both cancer cell lines improving the effect exerted by morin. To our knowledge, this is the first example of an oxovanadium complex with potent and selective activity against T47D and SKBR3 cancer cell lines. A similar improvement in the antitumor behavior of morin has been previously observed with its zinc and copper coordination complexes using human laryngeal epidermoid Hep-2 and baby hamster kidney BHK-21 cancer cell lines [51]. In this report the bioactive species were not identified and the inhibitory ratios were different between both complexes and the best effect was found for the copper one on the HL-60 cell line ($IC_{50} = 6.7 \times 10^{-5}$ M).

Considering the tumor-specific cytotoxicity in the tested breast tumor cell lines induced by morin and its oxovanadium(IV) complex, the antitumoral mechanism of action in these two cell lines was analyzed.

Like in the osteosarcoma cell line there is no appreciable ROS production in the cancer breast cells induced by morin or VOmor (even though they have been measured by two different methods in bone and breast tumor cells). The antioxidant *in vitro* measurements (see above) show that morin and VOmor are able to scavenge peroxyl and hydroxyl radicals, respectively and using this mechanism they can protect the cells from oxidative stress-induced cell death.

It is well known that cytochrome c is normally present inside the mitochondria. However, upon induction of apoptosis, the mitochondrial membrane potential is perturbed, which results in release of cytochrome c from the mitochondria to cytosol. This process leads to the activation of caspase-9 followed by the activation of caspase 3/7 and correlate with the result of apoptotic cell death. The results presented herein suggest that the pathway by which the newly synthesized VOmor complex induces apoptosis in the T47D and SKBR3 cell lines can be correlated with the activation of caspases 3/7 by means of the perturbation of the mitochondrial membrane potential. The damage in the plasmatic membrane has been examined measuring the amount of LDH release from the cytosol to the media (LDH assay). The plasmatic membrane has only been altered by the addition of VOmor in the SKBR3 cell line indicating that the effect of VOmor was sustained and translated in effect on cell viability in SKBR3. The results show that the treatment of the breast cancer cells with VOmor activates the apoptotic process in various steps along the death signaling pathway associated to the membrane potential perturbation, the caspase 3/7 activation and the damage of plasmatic membrane (in one of the cell lines).

The relatively higher sensitivity of SKBR3 cells to morin may be due to the activation of the apoptotic process through the perturbation of mitochondrial membrane potential and the activation of caspase 3/7 (in a lesser extent than its oxovanadium(IV) complex). Considering that oxovanadium(IV) cation do not significantly alter these parameters in the tested cell lines (data not shown) a mechanism different to the mitochondrial apoptotic pathway must be postulated for its deleterious effect in the SKBR3 cell line.

5. Conclusions

To verify the formation of a new morin–oxovanadium(IV) complex, Fourier transform IR, UV–vis, diffuse reflectance, EPR spectroscopies as well as elemental analysis and thermal measurements were performed. The $[VO(mor)_2H_2O]\cdot 5H_2O$ stoichiometry of the solid complex was assumed and we found that the coordination of the ligand to VO(IV) owed to the oxygen atoms of the carbonyl and hydroxyl moieties. We confirmed the formation of a 1:2 metal-to-ligand complex, in methanolic solution at pH 5, by UV–vis spectrophotometric titrations. These titrations were also followed by EPR spectroscopy and we can conclude that the conformation of single species would correspond to a similar binding mode like in the solid complex with an equatorial donor set of 2(C=O), 1(Ar–O^-) and a solvent molecule in the fourth position of the equatorial plane (*cis*-$VOL_2\cdot$EtOH). The solution studies allowed us to suggest that this is the active specie that exerted the biological effects. We were then able to discard other species in equilibrium and to perform direct comparisons between the solid and the dissolved complex. The antioxidant effect of 10 μM morin was determined and compared with bibliographic data. The complexation with $V(IV)O^{2+}$ improved the radical–scavenger activity for $OH^{\cdot}$ and O_2^{-}.

The proliferative effect of the osteoblastic cancer cell lines treated with specific concentrations of VOmor was significantly different to the antiproliferative effect exerted on the normal osteoblastic cells showing a non selective cytotoxicity. To test if the complex could induce selective cytotoxic effects against other cancer types, we evaluated the viability of breast cells (normal and tumoral) lines under the same concentrations. The tested breast cancer lines, T47D and SKBR3, were most sensitive to the deleterious effect of the complex. Morin and its oxovanadium(IV) complex showed *in vitro* antioxidant properties for different radicals and this may be the reason that they could assist in preventing ROS generation in both cancer cell types. The compounds did not cause DNA damage. Evidence indicates that the mechanism of the deleterious action on the breast tumor cell line may be due to the disruption of the mitochondrial membrane potential and to the activation of caspases 3/7 thus activating the apoptotic pathway. The *in vitro* antioxidant determinations against different free radicals including ROS are in accordance with the lack of production of ROS inside the cells discarding that the anticancer activity of these compounds is a consequence of a possible oxidative stress mechanism. Collectively, all the results of this study provide guidance for design structurally modified flavonoids with predominant bioactivities, improved antioxidant properties, tumor-specific cytotoxicities toward human breast cancer and selectivity between normal and tumoral cells.

Conflict of interest statement

The authors declare that there are no conflicts of interest.

Acknowledgements

This work was supported by UNLP, CONICET (PIP1125), ANPCyT (PICT 2008-2218) and CICPBA. EGF and SBE are members of the Carrera del Investigador, CONICET. PAMW is a member of the Carrera del Investigador CICPBA, Argentina. LN is a fellowship holder from CONICET.

References

[1] S.A. Aherne, N.M. O'Brien, Dietary flavonols: chemistry, Food Content Metab. Nutr. 18 (2002) 75–81.
[2] N.C. Cook, S. Samman, Flavonoids-chemistry, metabolism, cardioprotective effects, and dietary sources, J. Nutr. Biochem. 7 (1996) 66–76.
[3] J.W. Kim, J.H. Lee, B.Y. Hwang, S.H. Mun, N.Y. Ko, D.K. Kim, B. Kim, H.S. Kim, Y.M. Kim, W.S. Choi, Morin inhibits Fyn kinase in mast cells and IgE-mediated type I hypersensitivity response in vivo, Biochem. Pharmacol. 77 (2009) 1506–1512.
[4] W. Liu, R. Guo, Effects of Triton X-100 nanoaggregates on dimerization and antioxidant activity of morin, Mol. Pharm. 5 (2008) 588–597.
[5] V. Sivaramakrishnan, P.N.M. Shilpa, V.R.P. Kumar, S.N. Devaraj, Attenuation of *N*-nitrosodiethylamine-induced hepatocellular carcinogenesis by a novel flavonol-Morin, Chem. Biol. Interact. 171 (2008) 79–88.
[6] C.S. Yang, J.M. Landau, M.T. Huang, H.L. Newmark, Inhibition of carcinogenesis by dietary polyphenolic compounds, Annu. Rev. Nutr. 21 (2001) 381–406.
[7] P.C.H. Holiman, M.G.L. Hertog, M.B. Katan, Analysis and health effects of flavonoids, Food Chem. 57 (1996) 43–46.
[8] S. Subash, P. Subramanian, Effect of morin on the levels of circulatory liver markers and redox status in experimental chronic hyperammonaemic rats, Singapore Med. 49 (2008) 650–655.
[9] A. Evangelou, S. Karkabounas, G. Kalpouzos, M. Malamas, R. Liasko, D. Stefanou, A.T. Vlaho, T.A. Kabanos, Comparison of the therapeutic effects of two vanadium complexes administered at low doses on benzo[α]pyrene-induced malignant tumors in rats, Cancer Lett. 119 (1997) 221–225.
[10] T. Chakraborty, A. Chatterjee, A. Rana, D. Dhachinamoorthi, A. Kumar, M. Chatterjee, Carcinogen-induced early molecular events and its implication in the initiation of chemical hepatocarcinogenesis in rats: chemopreventive role of vanadium on this process, Biochim. Biophys. Acta 1772 (2007) 48–59.
[11] P. Villani, E. Cordelli, P. Leopardi, E. Siniscalchi, E. Veschetti, A.M. Fresegna, R. Crebelli, Evaluation of genotoxicity of oral exposure to tetravalent vanadium in vivo, Toxicol. Lett. 170 (2007) 11–18.
[12] D.X. Nguyen, P.D. Bos, J. Massagué, Metastasis: from dissemination to organ-specific colonization, Nat. Rev. Cancer 9 (2009) 274–284.
[13] M. Badea, R. Olar, D. Marinescu, V. Uivarosi, V. Aldea, T.O. Nicolescu, Thermal stability of new vanadyl complexes with flavonoid derivatives as potential insulin-mimetic agents, J. Therm. Anal. Calorim. 99 (2010) 823–827.
[14] M. Onishi, Photometric Determination of Traces of Metals, fourth ed., Wiley, New York, 1998. Part II.
[15] M.S. Islas, T. Rojo, L. Lezama, M. Griera Merino, M.A. Cortes, M. Rodriguez Puyol, E.G. Ferrer, P.A.M. Williams, Improvement of the antihypertensive capacity of candesartan and trityl candesartan by their SOD mimetic copper(II) complexes, J. Inorg. Biochem. 123 (2013) 23–33.
[16] A.M. Cortizo, S.B. Etcheverry, Vanadium derivatives act as growth factor-mimetic compounds upon differentiation and proliferation of osteoblast-like UMR106 cells, Mol. Cell. Biochem. 145 (1995) 97–102.
[17] C.M. Krejsa, S.G. Nadler, J.M. Esselstyn, T.J. Kavanagh, J.A. Ledbetter, G.L. Schieven, Role of oxidative stress in the action of vanadium phosphotyrosine phosphatase inhibitors. Redox independent activation of NF-kappaB, J. Biol. Chem. 272 (1997) 11541–11549.
[18] M.M. Bradford, A rapid and sensitive method for the quantitation of microgram quantities of protein utilizing the principle of protein–dye binding, Anal. Biochem. 72 (1976) 248–254.
[19] V.C. Sálice, A.M. Cortizo, C.L. Gómez Dumm, S.B. Etcheverry, Tyrosine phosphorylation and morphological transformation induced by four vanadium compounds on MC3T3E1 cells, Mol. Cell. Biochem. 198 (1999) 119–128.
[20] J.C. Cornard, J.C. Merlin, Spectroscopic and structural study of complexes of quercetin with Al(III), J. Inorg. Biochem. 92 (2002) 19–27.
[21] E.G. Ferrer, M.V. Salinas, M.J. Correa, L. Naso, D.A. Barrio, S.B. Etcheverry, L. Lezama, T. Rojo, P.A.M. Williams, Synthesis, characterization, antitumoral and osteogenic activities of quercetin vanadyl(IV) complexes, J. Biol. Inorg. Chem. 11 (2006) 791–801.
[22] Q.K. Panhwar, S. Memon, M.I. Bhanger, Synthesis, characterization, spectroscopic and antioxidation studies of Cu(II)–morin complex, J. Mol. Struct. 967 (2010) 47–53.
[23] S.B. Bukhari, S. Memon, M. Mahroof-Tahir, M.I. Bhanger, Synthesis, characterization and antioxidant activity copper–quercetin complex, Spectrochim. Acta A 71 (2009) 1901–1906.
[24] N.D. Chasteen, in: L.J. Berliner, J. Reuben (Eds.), Biological Magnetic Resonance, vol. 3, Plenum, New York, 1981.
[25] L. Naso, E.G. Ferrer, L. Lezama, T. Rojo, S.B. Etcheverry, P.A.M. Williams, Role of oxidative stress in the antitumoral action of a new vanadyl(IV) complex with the flavonoid chrysin in two osteoblast cell lines: relationship with the radical scavenger activity, J. Biol. Inorg. Chem. 15 (2010) 889–902.
[26] M. Musialik, R. Kuzmicz, T.S. Pawlowski, G. Litwinienko, Acidity of hydroxyl groups: an overlooked influence on antiradical properties of flavonoids, J. Org. Chem. 74 (2009) 2699–2709.
[27] M.W. Makinen, M.J. Brady, Structual origins of the insulin-mimetic activity of bis(acetylacetonato)oxovanadium(IV), J. Biol. Chem. 277 (2002) 12215–12220.
[28] S.B. Etcheverry, E.G. Ferrer, L.G. Naso, J. Rivadeneira, V. Salinas, P.A.M. Williams, Antioxidant effects of the VO(IV) hesperidin complex and its role in cancer chemoprevention, J. Biol. Inorg. Chem. 13 (2008) 435–447.
[29] P.C. Moorhouse, M. Grootveld, B. Halliwell, J.G. Quinlan, J.M.C. Guttetidge, Allopurinol and oxypurinol are hydroxyl radical scavengers, FEBS Lett. 213 (1987) 23–28.
[30] O. Potterat, Antioxidant and free radical scavengers of natural origin, Curr. Org. Chem. 1 (1997) 415–440.

[31] X. Shi, H. Jiang, Y. Mao, J. Ye, U. Saffiotti, Vanadium(IV)-mediated free radical generation and related 2′-deoxyguanosine hydroxylation and DNA damage, Toxicology 106 (1996) 27–38.
[32] M.A.M. Capella, L.S. Capella, R.C. Valente, M. Gefé, A.G. Lopes, Vanadate-induced cell death is dissociated from H_2O_2 generation, Cell. Biol. Toxicol. 23 (2007) 413–420.
[33] K. Lemanska, H. Szymusiak, B. Tyrakowska, R. Zielínskians, A.E.M.F. Soffers, I.M.C.M. Rietjens, The influence of pH on the antioxidant properties and the mechanisms of antioxidant action of hydroxyflavones, Free Radical Biol. Med. 31 (2001) 869–881.
[34] J.M. Herrero-Martínez, C. Repollés, E. Bosch, M. Rosés, C. Ráfols, Potentiometric determination of aqueous dissociation constants of flavonols sparingly soluble in water, Talanta 74 (2008) 1008–1013.
[35] R.H. Holm, P. Kennepohl, E.I. Solomon, Structural and functional aspects of metal sites in biology, Chem. Rev. 96 (1996) 2239–2314.
[36] E. Wóznicka, M. Kopacz, M. Umbreit, J. Kłos, New complexes of La(III), Ce(III), Pr(III), Nd(III), Sm(III), Eu(III) and Gd(III) ions with morin, J. Inorg. Biochem. 101 (2007) 774–782.
[37] P. Cos, L. Ying, M. Calomme, J.P. Hu, K. Cimanga, B. Van Poel, L. Pieters, A.J. Vlietinck, D. Vanden Berghe, Structure–activity relationship and classification of flavonoids as inhibitors of xanthine oxidase and superoxide scavengers, J. Nat. Prod. 61 (1998) 71–76.
[38] Q. Khan Panhwar, S. Memon, M.I. Bhanger, Synthesis, characterization, spectroscopic and antioxidation studies of Cu(II)–morin complex, J. Mol. Struct. 967 (2010) 47–53.
[39] A.M. Mendoza-Wilson, H. Santacruz-Ortega, R.R. Balandrán-Quintana, Relationship between structure, properties, and the radical scavenging activity of morin, J. Mol. Struct. 995 (2011) 134–141.
[40] S. Tachakittirungrod, F. Ikegami, S. Okonogi, Antioxidant active principles isolated from *Psidium guajava* grown in Thailand, Sci. Pharm. 75 (2007) 179–193.
[41] D. Villaño, M.S. Fernández-Pachón, M.L. Moyá, A.M. Troncoso, M.C. García-Parrilla, Radical scavenging ability of polyphenolic compounds towards DPPH free radical, Talanta 71 (2007) 230–235.
[42] A. Rice-Evans, N.J. Miller, G. Paganga, Structure–antioxidant activity relationships of flavonoids and phenolic acids, Free Biol. Med. 20 (1996) 933–956.
[43] K.G. Lee, T. Shibamoto, G.R. Takeoka, S.E. Lee, J.H. Kim, B.S. Park, Inhibitory effects of plant-derived flavonoids and phenolic acids on malonaldehyde formation from ethyl arachidonate, J. Agric. Food. Chem. 51 (2003) 7203–7207.
[44] R. Apak, K. Güçlü, B. Demirata, M. Özyürek, S.E. Çelik, B. Bektaşoğlu, K.I. Berker, D. Özyurt, Comparative evaluation of various total antioxidant capacity assays applied to phenolic compounds with the CUPRAC assay, Molecules 12 (2007) 1496–1547.
[45] N. Nenadis, L.F. Wang, M. Tsimidou, H.Y. Zhang, Estimation of scavenging activity of phenolic compounds using the $ABTS^{\cdot+}$ assay, J. Agric. Food Chem. 52 (2004) 4669–4674.
[46] D. Villaño, M.S. Fernández-Pachón, A.M. Troncoso, M.C. García-Parrilla, Comparison of antioxidant activity of wine phenolic compounds and metabolites in vitro, Anal. Chim. Acta 538 (2005) 391–398.
[47] Z. Cheng, J. Ren, Y. Li, W. Chang, Z. Chen, Study on the multiple mechansims underlying the reaction between hydroxyl radical and phenolic compounds by qualitative structure and activity relationship, Bioorg. Med. Chem. 10 (2002) 4067–4073.
[48] K.E. Heim, A.R. Tagliaferro, D.J. Bobilya, Flavonoid antioxidants: chemistry, metabolism and structure–activity relationships, J. Nutr. Biochem. 13 (2002) 572–584.
[49] C.D. Hapner, P. Deuster, Y. Chen, Inhibition of oxidative hemolysis by quercetin, but not other antioxidants, Chem. Biol. Interact. 186 (2012) 275–279.
[50] A. Chowdhury, K. Kishino, R. Satoh, K. Hashimoto, H. Kikuchi, H. Nishikawa, Y. Shirataki, H. Sakagami, Tumor-specificity and apoptosis-inducing activity of stilbenes and flavonoids, Anticancer Res. 25 (2005) 2055–2064.
[51] Z. Qi, W. Liufang, L. Xiang, L. Shuben, H. Fengying, Synthesis, characterization and antitumour properties of metal(II) solid complexes with Morin, Transition Met. Chem. 21 (1996) 23–27.